



HAL
open science

Exploring the impact of digestive physicochemical parameters of adults and infants on the pathophysiology of *Cryptosporidium parvum* using the dynamic TIM-1 gastrointestinal model

Julie Tottey, Lucie Etienne-Mesmin, Sandrine Chalançon, Alix Sausset, Sylvain Denis, Carine Mazal, Christelle Blavignac, Guillaume Sallé, Fabrice Laurent, Stéphanie Blanquet-Diot, et al.

► To cite this version:

Julie Tottey, Lucie Etienne-Mesmin, Sandrine Chalançon, Alix Sausset, Sylvain Denis, et al.. Exploring the impact of digestive physicochemical parameters of adults and infants on the pathophysiology of *Cryptosporidium parvum* using the dynamic TIM-1 gastrointestinal model. *Gut Pathogens*, 2024, 16 (1), pp.55. 10.1186/s13099-024-00648-2 . hal-04722156

HAL Id: hal-04722156

<https://hal.science/hal-04722156v1>

Submitted on 4 Oct 2024

HAL is a multi-disciplinary open access archive for the deposit and dissemination of scientific research documents, whether they are published or not. The documents may come from teaching and research institutions in France or abroad, or from public or private research centers.

L'archive ouverte pluridisciplinaire **HAL**, est destinée au dépôt et à la diffusion de documents scientifiques de niveau recherche, publiés ou non, émanant des établissements d'enseignement et de recherche français ou étrangers, des laboratoires publics ou privés.



Distributed under a Creative Commons Attribution - NonCommercial - NoDerivatives 4.0 International License

RESEARCH

Open Access



Exploring the impact of digestive physicochemical parameters of adults and infants on the pathophysiology of *Cryptosporidium parvum* using the dynamic TIM-1 gastrointestinal model

Julie Totley^{1*}, Lucie Etienne-Mesmin², Sandrine Chalançon², Alix Sausset¹, Sylvain Denis², Carine Mazal², Christelle Blavignac³, Guillaume Sallé¹, Fabrice Laurent¹, Stéphanie Blanquet-Diot² and Sonia Lacroix-Lamandé¹

Abstract

Background Human cryptosporidiosis is distributed worldwide, and it is recognised as a leading cause of acute diarrhoea and death in infants in low- and middle-income countries. Besides immune status, the higher incidence and severity of this gastrointestinal disease in young children could also be attributed to the digestive environment. For instance, human gastrointestinal physiology undergoes significant changes with age, however the role this variability plays in *Cryptosporidium parvum* pathogenesis is not known. In this study, we analysed for the first time the impact of digestive physicochemical parameters on *C. parvum* infection in a human and age-dependent context using a dynamic in vitro gastrointestinal model.

Results Our results showed that the parasite excystation, releasing sporozoites from oocysts, occurs in the duodenum compartment after one hour of digestion in both child (from 6 months to 2 years) and adult experimental conditions. In the child small intestine, slightly less sporozoites were released from excystation compared to adult, however they exhibited a higher luciferase activity, suggesting a better physiological state. Sporozoites collected from the child jejunum compartment also showed a higher ability to invade human intestinal epithelial cells compared to the adult condition. Global analysis of the parasite transcriptome through RNA-sequencing demonstrated a more pronounced modulation in ileal effluents compared to gastric ones, albeit showing less susceptibility to age-related digestive condition. Further analysis of gene expression and enriched pathways showed that oocysts are highly active in protein synthesis in the stomach compartment, whereas sporozoites released in the ileum showed downregulation of glycolysis as well as strong modulation of genes potentially related to gliding motility and secreted effectors.

Conclusions Digestion in a sophisticated in vitro gastrointestinal model revealed that invasive sporozoite stages are released in the small intestine, and are highly abundant and active in the ileum compartment, supporting reported

*Correspondence:

Julie Totley
julie.totley@inrae.fr

Full list of author information is available at the end of the article



© The Author(s) 2024. **Open Access** This article is licensed under a Creative Commons Attribution-NonCommercial-NoDerivatives 4.0 International License, which permits any non-commercial use, sharing, distribution and reproduction in any medium or format, as long as you give appropriate credit to the original author(s) and the source, provide a link to the Creative Commons licence, and indicate if you modified the licensed material. You do not have permission under this licence to share adapted material derived from this article or parts of it. The images or other third party material in this article are included in the article's Creative Commons licence, unless indicated otherwise in a credit line to the material. If material is not included in the article's Creative Commons licence and your intended use is not permitted by statutory regulation or exceeds the permitted use, you will need to obtain permission directly from the copyright holder. To view a copy of this licence, visit <http://creativecommons.org/licenses/by-nc-nd/4.0/>.

C. parvum tissue tropism. Our comparative analysis suggests that physicochemical parameters encountered in the child digestive environment can influence the amount, physiological state and possibly invasiveness of sporozoites released in the small intestine, thus potentially contributing to the higher susceptibility of young individuals to cryptosporidiosis.

Keywords *Cryptosporidium*, Apicomplexa, In vitro digestive model, Physicochemical parameters, Child and adult digestion

Background

The zoonotic disease cryptosporidiosis caused by the apicomplexan parasite *Cryptosporidium* is endemic in many low-income countries and potentially epidemic in high-income countries. This enteric disease leads to watery diarrhoea that can be life-threatening in individuals with an immature or a compromised immune system. Results from cohort studies have consistently shown that young age is associated with a higher risk of *Cryptosporidium* infection [1]. Accordingly, *Cryptosporidium* infection is particularly associated with prolonged (7–14 days) or even persistent (≥ 14 days) diarrhoea during childhood, and can also lead to malnutrition and growth deficiency [1]. Cryptosporidiosis is considered as one of the most common causes of infectious moderate-to-severe diarrhoea in children under the age of two [2, 3] and an important contributor to early childhood mortality in low-resource settings [4], thus constituting a serious public health concern. In 2016, acute infections due to *Cryptosporidium* caused more than 48,000 deaths in children under 5 years and more than 4.2 million disability-adjusted life-years lost [5].

Cryptosporidium parvum is one of the two most relevant *Cryptosporidium* species to humans and is transmitted primarily by the fecal–oral route either by direct contact with an infected human or animal or indirectly via food or water contaminated by oocysts [6]. Once ingested, *C. parvum* oocysts excyst in the gastrointestinal tract, releasing infective and motile sporozoites that invade intestinal epithelial cells. The parasite life cycle then progresses through three rounds of asexual replication [7] before shifting to sexual reproduction and then to the production of a high number of infectious oocysts that ensure either auto-infection of the same host by infecting nearby intestinal cells or transmission in the environment after release in the faeces.

The higher incidence and severity of cryptosporidiosis reported in children under the age of two can be first attributed to their immature immune status, making them as susceptible to the infection by the parasite as immunocompromised adults [8]. Nevertheless, other factors, such as those associated with the digestive environment (i.e., immaturity of digestive processes, intestinal epithelium and resident microbiota) where *C. parvum* infection takes place, could also contribute to the age-dependent nature of symptomatic cryptosporidiosis.

Consequently, there is a crucial need to investigate *C. parvum* pathogenesis considering the gastrointestinal physiology that varies greatly with age [9], especially in light of the differences in digestive physicochemical parameters encountered in children, compared to adults.

Due to obvious ethical and technical reasons, it remains very difficult to evaluate the pathophysiology of food- or water-borne pathogens in the human gastrointestinal tract, especially in pediatric populations. In vitro gastrointestinal models represent an appropriate alternative to in vivo assays to study the impact of digestive physicochemical parameters alone (i.e., independently of any other influencing factors from the host) in a nutritional, pharmaceutical, toxicological or microbiological context. Among the available gastrointestinal systems, the computer-controlled TNO (Toegepast Natuurwetenschappelijk Onderzoek) gastroIntestinal Model-1 (TIM-1), which combines multi-compartmentalisation and dynamism, is one of the most complete in vitro simulators of the human upper gastrointestinal tract [10]. By reproducing physiologically relevant conditions, the TIM-1 system allows the closest simulation of in vivo dynamic events occurring within the human stomach and three compartments of the small intestine. As a result, it has been successfully used in diverse applications in the past, for instance in an array of pathogen-related microbiological studies [10–16]. As an example, the TIM-1 model has been used to demonstrate that the variability in human digestive physicochemical parameters that occurs between child and adult populations could play a role in *E. coli* O157:H7 pathogenesis, which is considerably more severe in children than in adults [12].

Within this framework, we designed an original approach to determine for the first time the impact of digestive physicochemical parameters on *C. parvum* infection, in a human and age-dependent context. The aim of the present study was to use the sophisticated TIM-1 model for a comparative analysis of *C. parvum* infection under the digestive conditions encountered in young children (from 6 months to 2 years) or in adults following the simulated digestion of a glass of contaminated water. Various parasite parameters, from the parasite excystation kinetics and global gene expression, to the sporozoite physiological state and infectivity, were monitored throughout the simulated human digestions.

Methods

Cells and parasites

Human ileocecal adenocarcinoma cells (HCT-8) were purchased from the American Type Culture Collection, cultured in RPMI 1640 with phenol red supplemented with 2 mM GlutaMAX™, 10% (v/v) heat-inactivated fetal bovine serum (FBS), 1 mM sodium pyruvate, 50 U/ml penicillin, and 50 µg/ml streptomycin and maintained at 37 °C in a humidified atmosphere under 5% CO₂. The *C. parvum* INRAE Nluc strain was generated by transgenesis to produce Nluc-expressing parasites, and purified as described in Swale et al., 2019 [17].

In vitro digestions in the TIM-1 gastrointestinal model

The TIM-1 model (TNO, Zeist, The Netherlands) consists of four successive compartments simulating the human stomach and the three segments of the small intestine (duodenum, jejunum, and ileum) (Fig. 1). The main parameters of digestion, such as body temperature, pH, peristaltic mixing and transport, gastric, biliary, and pancreatic secretions and passive

absorption of small molecules and water, are reproduced as accurately as possible, as already described [16]. The TIM-1 system was programmed as described in Table 1 to reproduce, based on in vivo data, the digestive conditions observed in a healthy adult or a young child (from 6 months to 2 years) when a glass of water is ingested. The TIM-1 system was inoculated with a parasite suspension consisting of 200 mL of mineral water (Volvic®, Danone, France) experimentally contaminated with 1×10^8 oocysts of the *C. parvum* INRAE Nluc strain. Two sets of experiments were performed: gastric digestions where the stomach compartment was solely used (total duration of 60 min) and gastrointestinal digestions using the entire TIM-1 model (total duration of 300 min). Digestions were run in triplicate.

TIM-1 sampling

Samples were taken in the initial parasite suspension ($t=0$) and regularly collected during in vitro digestions from each digestive compartment (stomach,

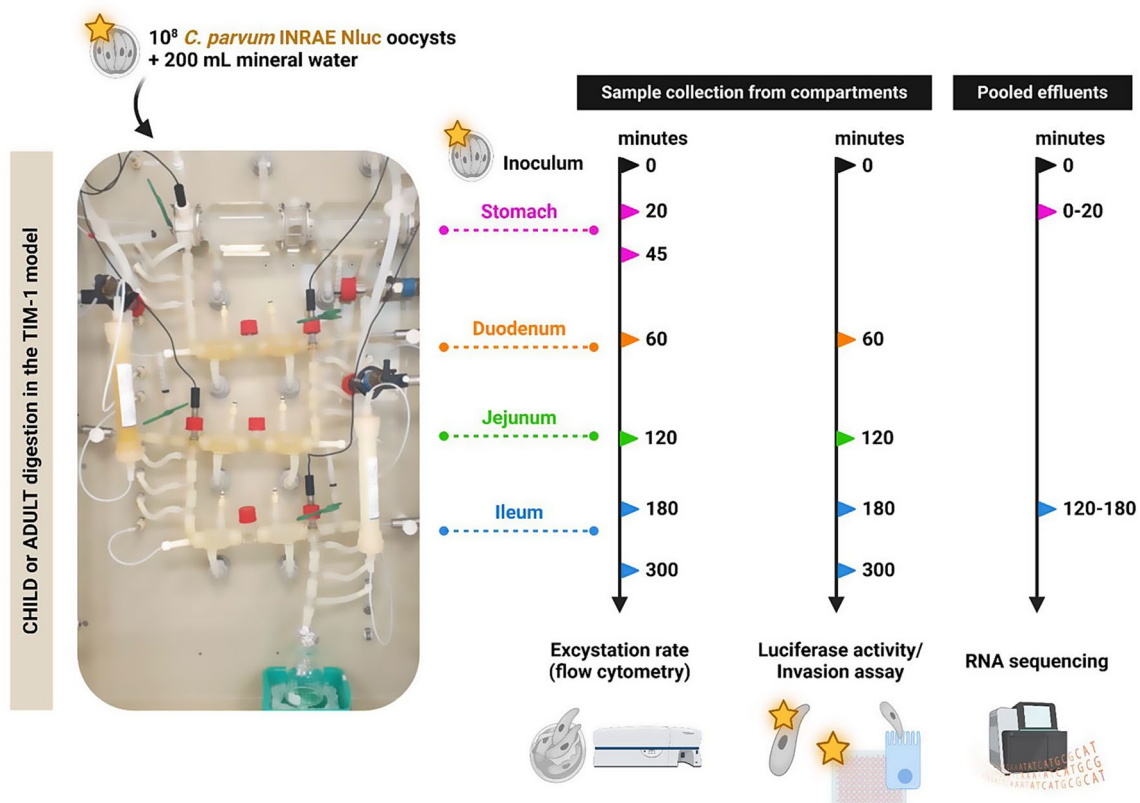


Fig. 1 TIM-1 experimental set-up and analysis. The left side shows a picture of the TIM-1 system composed of four successive compartments simulating the human stomach and the three parts of the small intestine (i.e., the duodenum, jejunum and ileum) mimicking the main physicochemical parameters of human gastrointestinal digestion. Digestion experiments were performed to reproduce an adult or an infant (from 6 months old to 2 years old) ingesting a glass of water contaminated with 1×10^8 oocysts of the *C. parvum* INRAE Nluc strain. On the right side, sampling times (minutes) are indicated when samples were taken either directly from each compartment (for flow cytometry, sporozoite luciferase activity and invasion assay); or indirectly by pooling the gastric effluents when the stomach compartment was solely used, or the ileal effluents when the entire TIM-1 system was used (for RNA sequencing). Digestions were run in triplicate. Created with BioRender.com (Agreement number: JH26ZFM4TU)

Table 1 Parameters of gastrointestinal digestion in the TIM-1 system under adult or infant conditions

| Parameter | Adult | Infant |
|---|--|--|
| pH | Gastric compartment (min/pH) | Gastric compartment (min/pH) |
| | t = 10 → 3.2 | t = 10 → 5.7 |
| | t = 20 → 2.4 | t = 20 → 5.3 |
| | t = 40 → 1.8 | t = 40 → 4.5 |
| | t = 60 → 1.6 | t = 60 → 3.2 |
| | t = 90 → 1.5 | t = 90 → 2.0 |
| | Duodenal compartment: 6.4 | Duodenal compartment: 6.4 |
| | Jejunal compartment: 6.9 | Jejunal compartment: 6.9 |
| | Ileal compartment: 7.2 | Ileal compartment: 7.2 |
| | Digestive secretions | Gastric compartment |
| 130 IU/min of pepsin | | 130 IU/min of pepsin |
| 10 IU/min of lipase | | 10 IU/min of lipase |
| 0 to 0.25 mL/min of HCl 0.5 M (according to pH) | | 0 to 0.25 mL/min of HCl 0.3 M (according to pH) |
| Duodenal compartment | | |
| 1 mL/min Bile salts ^a 27.9 mM during the first 30 min and then 9.3 mM | | 1 mL/min Bile salts ^a 14 mM during the first 30 min, then 4.67 mM |
| 0.5 mL/min Pancreatin 4USP juice 44.6 g/L | | 0.5 mL/min Pancreatin 4USP juice 22.3 g/L |
| Trypsin ^b : 3 mg | | Trypsin ^b : 2.4 mg |
| 0.5 mL/min of intestinal electrolytes solution ^c combined to NaHCO ₃ 0.5 mol/L if necessary (according to pH) | | 0.5 mL/min of intestinal electrolytes solution combined to NaHCO ₃ 0.5 mol/L if necessary (according to pH) |
| Jejunal compartment | | |
| 0 to 0.25 mL/min of NaHCO ₃ 0.5 mol/L (according to pH) | 0 to 0.25 mL/min of NaHCO ₃ 0.5 mol/L (according to pH) | |
| Ileal compartment | | |
| 0 to 0.25 mL/min of NaHCO ₃ 0.5 mol/L (according to pH) | 0 to 0.25 mL/min of NaHCO ₃ 0.5 mol/L (according to pH) | |

^aBile is composed of a mixture of bile extract porcine and bile salts (sodium deoxycholate and sodium cholate hydrate)

^bintroduced into the duodenum compartment at t=0

^cElectrolytes solution is composed of 7 g/l NaCl, 0.6 g/l KCl, and 0.3 g/l CaCl₂ dihydrate

duodenum, jejunum, and ileum) to evaluate parasite excystation kinetics, sporozoite luciferase activity and host cell invasion (Fig. 1). Gastric and ileal effluents were also collected on ice and pooled on 0–20, 20–45, and 45–60 min for gastric digestions and hour-by-hour during 5 h for gastrointestinal digestions. Gastric and ileal effluents collected during 0–20 min and 120–180 min, respectively, were used for RNA extraction.

Parasite excystation kinetics

The parasite excystation success was monitored in three independent experiments by flow cytometry from samples collected regularly from each digestive compartment during in vitro digestions in the TIM-1 system. Prior to each TIM-1 digestion assay, flow cytometry controls and gating strategy on forward-angle light scatter/side-angle light scatter were performed based on analysis of intact (non-excysted) oocysts, and non-filtered or 5 µm-filtered (Sartorius AG, Göttingen, Germany) in vitro excysted parasites (Fig. 2.A). Such controls aimed to differentiate *C. parvum* oocysts from sporozoites and from the background. Flow cytometry analyses were all performed immediately after sample collection on a BD™ LSR II cytometer and data were collected with the BD FACSDiva™ Software version 9 (BD Biosciences, Franklin Lakes, USA). Results are expressed as relative percentages of parasites detected as intact oocyst stages in each digestive compartment compared to the corresponding age condition's inoculum.

Sporozoite luciferase activity

The physiological state of *C. parvum* sporozoites was monitored in three independent experiments for the initial parasite suspension and for samples collected regularly from the duodenum, jejunum and ileum compartments during in vitro digestions in the TIM-1 system. Immediately after collection, each sample was washed with phosphate-buffered saline (PBS), filtered through a 5 µm membrane (Sartorius AG, Göttingen, Germany) to discard oocysts and empty shells, centrifuged (10000 × g, 3 min, 4 °C) and resuspended in PBS. The luciferase activity expressed by the recovered sporozoites was assessed (three replicates for each sample) using the Nano-Glo® Luciferase Assay System (Promega Corporation, Madison, USA). The sporozoites were mixed (v/v) with the Nano-Glo® Luciferase Assay Buffer containing 1:50 of the Nano-Glo® Luciferase Assay Substrate and the luminescence was measured with the GloMax®-Multi Detection System (Promega Corporation, Madison, USA). The luciferase activity expressed by sporozoites collected from the TIM-1 compartments was normalised to the initial parasite suspension for each assay.

Parasite invasion assay

The ability of *C. parvum* sporozoites to invade intestinal epithelial cells was monitored in two independent experiments for samples collected regularly from the small intestinal compartments during in vitro digestions. Immediately after collection, each parasite sample was washed with sterile PBS, filtered through a 5 µm membrane (Sartorius AG, Göttingen, Germany) to discard oocysts and empty shells, centrifuged (10000 × g, 3 min, 4 °C) and resuspended into sterile PBS. The recovered

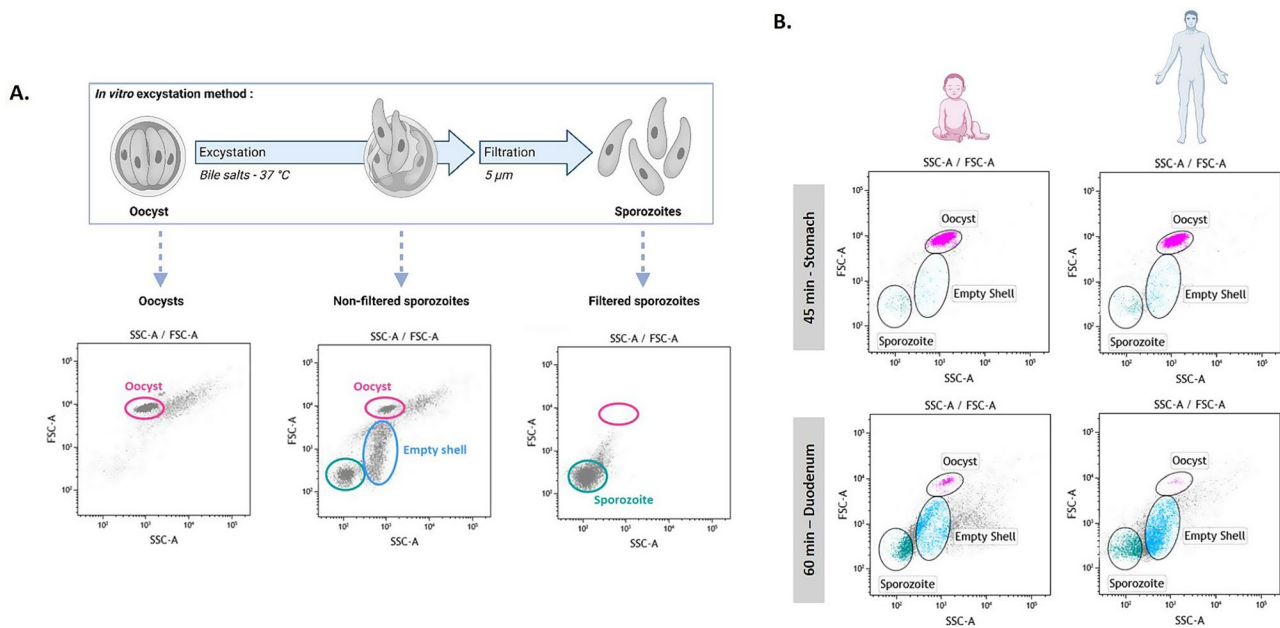


Fig. 2 *Cryptosporidium parvum* excystation in the human in vitro upper gastrointestinal tract. **(A)** Flow cytometry gating strategy on forward-angle light scatter/side-angle light scatter established during in vitro excystation of parasites, allowing detection of intact oocysts, empty oocyst shells and sporozoites. Created with BioRender.com (Agreement number: FF26ZFMVSM). **(B)** Parasite excystation during child or adult digestion in the TIM-1 system. Cytograms obtained for one representative experiment for the child or the adult digestion at 45 min in the stomach and at 60 min in the duodenum show the timing when excystation occurs in the in vitro gastrointestinal tract

sporozoites were immediately used to infect HCT-8 cell monolayers grown to 80% confluence in Nunc™ F96 MicroWell™ white polystyrene plates (Thermo Fisher Scientific, Waltham, USA). After 2.5 h, cells were washed twice with sterile PBS and used to analyse the invasion of parasites (six replicates per sample). The luciferase activity was detected directly from the infected cell monolayers using the Nano-Glo® Luciferase Assay System (Promega Corporation, Madison, USA) and the GloMax®-Multi Detection System as described above. Luciferase activity data were normalised to the luminescence background detected in uninfected cultures.

Parasite RNA extraction

RNA samples were collected on ice from the initial parasite suspension and from gastric (0–20 min) or ileal (120–180 min) effluents during in vitro digestions. Samples were then centrifuged ($10000 \times g$, 5 min, 4 °C), resuspended into 500 µL TRI Reagent® (Sigma-Aldrich, Saint-Louis, USA) and subjected to 5 cycles of [1 min vortexing – 1 min on ice] after addition of 0.5 mm glass beads. The lysates were centrifuged ($10000 \times g$, 10 min, 4 °C) and the supernatants were mixed with absolute ethanol and transferred to a Zymo-Spin™ IC column (Direct-zol™ RNA Microprep kit, Zymo Research, Irvine, USA). Total RNAs were isolated according to the manufacturer's instructions. Any contaminating genomic DNA was removed using the DNase I Set kit (Zymo Research). RNA was further purified with the RNA Clean

& Concentrator™-5 kit (Zymo Research) and concentrations measured using the Qubit™ 2.0 fluorometer using RNA HS assay kit (Thermo Fisher Scientific). RNA quality was assessed using the Agilent 2100 Bioanalyzer system and the RNA 6000 Pico kit (Agilent Technologies, Santa Clara, USA).

RNA-Seq analysis of differentially expressed genes

Library construction and sequencing were performed by Helixio (Biopôle Clermont-Limagne, Saint-Beauzire, France). The RNA library preparation was performed using the QuantSeq 3' mRNA-Seq Library Prep Kit FWD for Illumina (Lexogen, Vienna, Austria). A total of 15 RNA-Seq libraries were generated, corresponding to 3 libraries for each experimental group, and then sequenced with the NextSeq® 500 System (Illumina, San Diego, USA) using a single-read sequencing of 76 bp length configuration. Raw sequence data were assessed for quality using the FastQC v0.11.3 tool (Babraham Institute, Cambridge, UK). Sequenced reads were aligned to the *C. parvum* IOWA-ATCC reference genome (genome assembly ID: ASM1524537v1) using the STAR software [18]. The number of sequences reads that mapped the *C. parvum* genome varied between 11 and 14 million per library. Gene counts were determined using the STAR software. The R-based packages DESeq2 [19] and edgeR [20] were used to normalise data, perform descriptive analysis as well as all pairwise comparisons to determine the differentially expressed genes between

experimental groups. Clustering of transcriptomic profiles was assessed through a principal-component analysis (PCA) using normalised RNA-Seq data of a set of 2430 filtered genes, for which at least 10 reads were counted in a minimum of three samples. The *P*-values generated during pairwise comparisons were adjusted for multiple testing with the Benjamini-Hochberg procedure which controls for false discovery rate (FDR). Genes were considered to be differentially expressed between two experimental groups at an FDR adjusted *P*-value < 0.05. Gene Ontology (GO) [21, 22] and KEGG Metabolic Pathway [23–25] enrichment analyses were performed on differentially expressed genes on CryptoDB [26].

Statistical analysis

Graphs and boxplots were generated using GraphPad Prism version 10.2.3 and statistical analyses were performed using R version 4.3.1. Significant differences in luciferase activity and invasion ability data according to time of digestion were tested using a nonparametric analysis of longitudinal data with the R package “nparLD” [27] version 2.2. In case of a significant time effect, pairwise comparisons between time points were calculated with the R package “nparcomp” [28] version 3.0. *P* < 0.05 was considered statistically significant and indicated by non-corresponding letters (lowercase for the child condition and capitals for the adult condition). The Mann-Whitney non-parametric test was performed to test the effect of treatment (child vs. adult) for each time point and to analyse luciferase data collected from live or heat-killed parasites (Additional file 1), with significant differences indicated as follows: * *P* < 0.05; ** *P* < 0.01; *** *P* < 0.001; **** *P* < 0.0001.

Results

Parasite excystation kinetics in the simulated upper gastrointestinal tract

To establish the gating strategy, flow cytometry controls were performed during in vitro excystation of parasites (Fig. 2.A). These controls showed that intact oocysts were abundant before excystation and easily discriminated from empty shells and sporozoites during the process of excystation (when non-filtered). In contrast, intact

oocysts were scarcely detected in filtered excysted samples, in which mostly sporozoites could be observed.

The same gating strategy was then used to monitor parasite excystation kinetics during child and adult digestions in the TIM-1 system. Time of digestion had an overall significant effect on parasite excystation in both child (*P* < 0.0001) and adult (*P* < 0.0001) conditions. In the simulated stomach compartment, the proportion of intact oocysts (i.e., non-excysted parasites) remained high regardless of the age condition, with $80.4 \pm 7.2\%$ and $81.4 \pm 10.1\%$ intact oocysts detected at 45 min for child and adult digestion, respectively (Fig. 2.B, Table 2). In contrast, subsequent transit in the duodenal compartment marked a brutal decrease in the proportion of intact oocysts detected, which dropped to $4.5 \pm 0.3\%$ and $1.5 \pm 0.3\%$ at 60 min for child and adult condition, respectively. The parasite excystation further progressed in the small intestine compartments and reached a minimal amount of intact oocysts detected for both conditions in the ileal compartment by the end of digestion ($1.0 \pm 0.1\%$ and $0.6 \pm 0.1\%$ at 300 min for the child and the adult digestion, respectively). The quantity of intact oocysts detected in the child's small intestine was consistently higher when compared to the adult condition whatever the compartment and time considered (Table 2). Our results suggest that sporozoites released from excystation in the small intestine would be slightly less abundant in infants compared to adults.

The parasite excystation kinetics was analysed by flow cytometry during child or adult digestion in the TIM-1 system. Samples recovered from the inoculum (Ino) or from the stomach (Sto), duodenum (Duo), jejunum (Jej) or ileum (Ile) compartments were immediately processed after collection. Values from three independent child or adult digestion in the TIM-1 system are expressed as relative percentages of intact oocysts as compared with that of the inoculum for each digestion assay.

Physiological state and invasion ability of *C. Parvum* sporozoites collected from the in vitro small intestine

The physiological state of the sporozoites released following excystation in the small intestine of the TIM-1 system was estimated through analysis of the activity of the luciferase reporter gene that is constitutively expressed by the

Table 2 Percentage of parasites detected as intact oocysts for the child or adult TIM-1 experiments

| Age condition | TIM-1 digestion | 0 min Ino | 20 min Sto | 45 min Stomach | 60 min Duo | 120 min Jej | 180 min Ile | 300 min Ile |
|---------------|-----------------|--------------|---------------|-------------------|---------------|----------------|----------------|----------------|
| Child | 1 | 100 | 98.2 | 93.5 | 3.8 | 1.9 | 1.8 | 1.1 |
| | 2 | 100 | 73.5 | 68.6 | 4.7 | 2.6 | 2.4 | 0.9 |
| | 3 | 100 | 86.8 | 79.0 | 5.0 | 2.7 | 2.6 | 1.0 |
| Adult | 1 | 100 | 101.5 | 99.5 | 1.4 | 1.3 | 1.2 | 0.9 |
| | 2 | 100 | 83.2 | 64.7 | 2.0 | 1.4 | 1.1 | 0.6 |
| | 3 | 100 | 90.1 | 79.9 | 1.0 | 0.7 | 0.6 | 0.4 |

parasite strain (Fig. 3.A). Time of digestion had an overall significant effect on sporozoite luciferase activity in both child ($P < 0.0001$) and adult ($P < 0.0001$) conditions. In the child small intestine, sporozoite relative luciferase activity significantly increased from 38.9 ± 12.1 normalised

relative light units (RLUs) in the duodenum at 60 min and 950.5 ± 12.1 RLUs in the jejunum at 120 min to a maximum reached at 180 min in the ileum ($2.0 \times 10^4 \pm 4.2 \times 10^3$ RLUs; $P < 0.0001$ between 60 min and 180 min and between 120 min and 180 min). During the last two

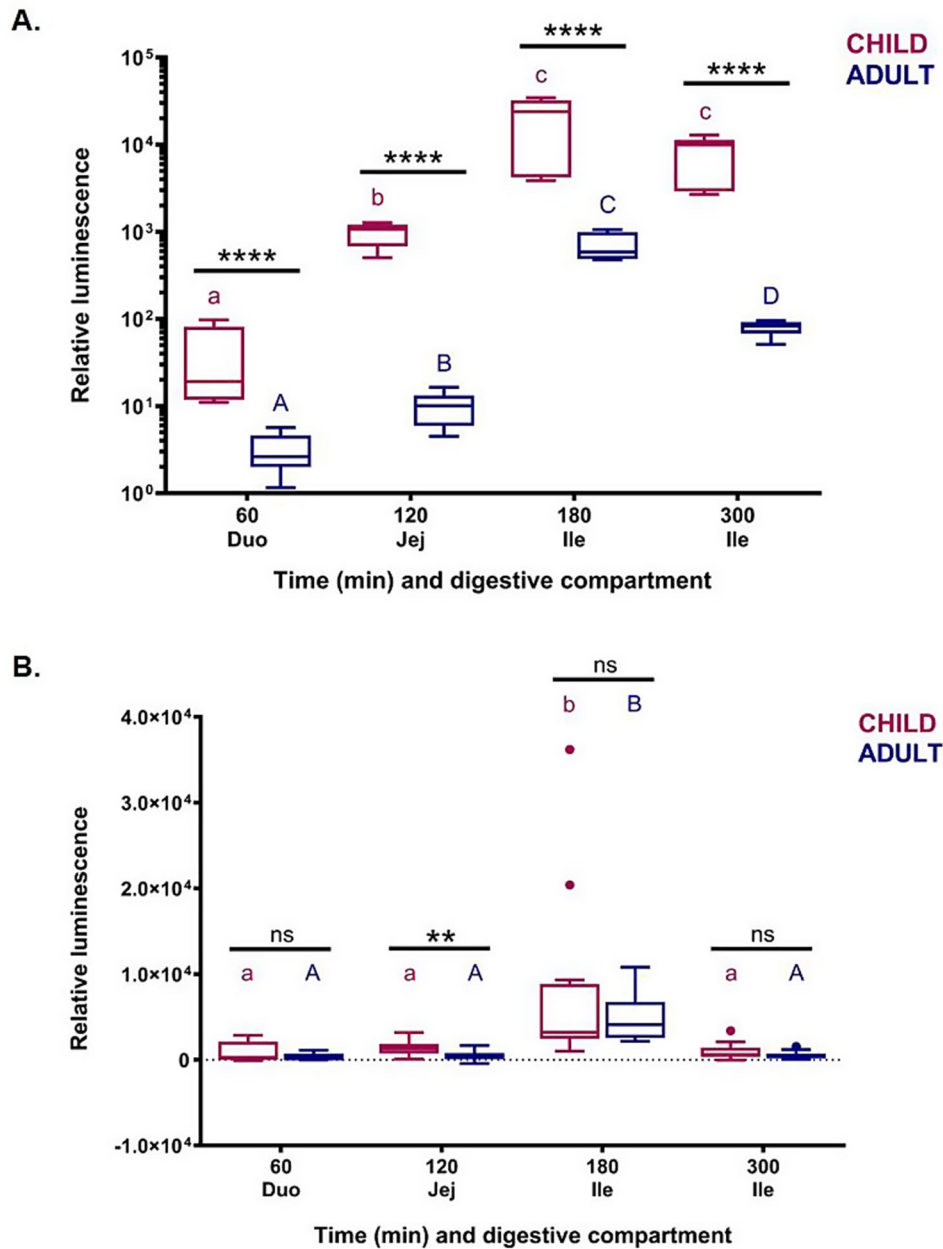


Fig. 3 Physiological state and invasion ability of *Cryptosporidium parvum* sporozoites collected from the TIM-1 system. **(A)** Luciferase activity expressed by *C. parvum* sporozoites collected from the duodenal (Duo), jejunal (Jej) or ileal (Ile) TIM-1 compartments during child (purple) or adult (dark blue) digestion. Boxplots depict the relative luminescence of sporozoites compared with that of the inoculum for each digestion assay. For each age condition, significant differences ($P < 0.05$) between time points are indicated by non-corresponding letters (purple lowercase for child digestion and blue capitals for adult digestion). For each time point, significant differences between age conditions are indicated in black as follows: **** $P < 0.0001$. **(B)** Invasion assay. *C. parvum* sporozoites were allowed to infect HCT-8 monolayers for 2.5 h before evaluation of luminescence intensity. Boxplots depict the luminescence measured in infected cells from which the luciferase background measured in non-infected cells has been removed. For each age condition, significant differences ($P < 0.01$ or $P < 0.001$ for child or adult, respectively) between time points are indicated by non-corresponding letters (purple lowercase for child digestion and blue capitals for adult digestion). For each time point, significant differences between age conditions are indicated in black as follows: ** $P < 0.01$

hours of digestion, the relative luciferase activity detected in the child ileal compartment decreased ($7.9 \times 10^3 \pm 1.4 \times 10^3$ RLUs) but remained significantly higher than the one detected in the duodenum and jejunum at the beginning of digestion ($P < 0.0001$ between 60 min and 300 min and between 120 min and 300 min). The luciferase activity kinetics of sporozoites collected from the adult digestions followed the same trend but at a much lower intensity, with a maximum reached of 706.7 ± 80.0 RLUs at 180 min in the ileum. Additionally, the relative luciferase activity expressed by sporozoites was consistently and significantly higher for the child condition when compared to the adult one, whatever the compartments of the small intestine and the time points ($P < 0.0001$ at 60, 120, 180 and 300 min). Controls performed on the *C. parvum* INRAE Nluc strain showed that the luciferase activity measured from excysted parasites was dependent on the quantity ($P < 0.01$ between 1×10^7 and 1×10^8 excysted parasites) and viability ($P < 0.01$ between live and heat-killed parasites) of parasites present in the sample (Additional file 1). In the TIM-1 small intestine under child condition, fewer sporozoites (Fig. 2.B, Table 2) but a significantly higher luciferase activity (Fig. 3.A) was detected compared to the adult condition.

The invasion ability of Nluc-expressing sporozoites collected and purified from the TIM-1 small intestine was assessed by in vitro infection of HCT-8 cell monolayers and subsequent determination of luciferase activity (Fig. 3.B). Time of digestion had an overall significant effect on sporozoite ability to invade host cells in both child ($P < 0.0001$) and adult ($P < 0.0001$) conditions. The invasion of HCT-8 monolayers was observed to be low and stable for sporozoites collected from the duodenum at 60 min or from the jejunum at 120 min of both child ($9.3 \times 10^2 \pm 3.4 \times 10^2$ RLUs and $1.4 \times 10^3 \pm 2.5 \times 10^2$ RLUs, respectively) and adult ($3.0 \times 10^2 \pm 1.2 \times 10^2$ RLUs and $4.6 \times 10^2 \pm 1.6 \times 10^2$ RLUs, respectively) digestive conditions. The invasion ability was observed to be significantly increased for sporozoites collected at 180 min from the child ileum ($8.0 \times 10^3 \pm 3.0 \times 10^3$ RLUs; $P < 0.01$ between 180 min and other time points) or the adult ileum ($4.8 \times 10^3 \pm 8.0 \times 10^2$ RLUs; $P < 0.0001$ between 180 min and other time points). By the end of digestion, parasite invasion dropped to a level comparable to the one observed at 60–120 min, with a relative luminescence of $1.0 \times 10^3 \pm 2.8 \times 10^2$ or $5.1 \times 10^2 \pm 1.3 \times 10^2$ RLUs detected for monolayers infected with sporozoites collected at 300 min in the child or adult ileum, respectively. The invasion ability of sporozoites was significantly higher in children compared with adults only at 120 min in the jejunum ($P < 0.01$).

Parasite gene expression following child or adult digestion in the TIM-1 model

The parasite transcriptome modifications induced by adult or child digestions in the TIM-1 were determined by whole transcriptome sequencing (RNA-Seq) for gastric (0–20 min) and ileal (120–180 min) effluents, and also for the initial inoculum as control. A principal component analysis (PCA) was performed to evaluate the samples' distribution according to their expression profiles. The first (31%) and second (16%) components represented most of the differential expression pattern with a cumulative proportion of 47% (Fig. 4.A). This PCA analysis revealed a segregation between samples collected at different time points and from different TIM-1 compartments. The PCA plot showed that all six samples from the ileal effluents were grouped together, and that the three inoculum samples and the six samples from the gastric effluents formed two other distinct groups (i.e., clusters), despite samples 'Inoculum_3' and 'Stomach_Adult2' being more distant from their respective replicates. For each cluster corresponding to samples collected from gastric or ileal effluents, no further segregation by age could be observed, suggesting that most of the variance is explained by time and/or digestive compartment, rather than simulated age (i.e., child vs. adult). Indeed, pairwise comparisons resulted in no or only one gene (Gene ID CPATCC_0017110: unspecified product) whose expression was significantly modified (i.e., showing an adjusted P -value [FDR] < 0.05 and a minimum 2-fold regulation [$\log_2FC > 1$]) between the two age conditions when effluent was collected in the gastric or in the ileal compartment, respectively (Fig. 4.B, Additional files 2 and 3). In contrast, expression profiles were more affected by time and/or digestive compartment, with for example 22 genes whose transcription levels were modified between gastric samples and inoculum for both age conditions, and 83 or 99 genes between gastric and ileal samples for child or adult conditions, respectively. Furthermore, the strongest modulation of the parasite transcriptome was observed between ileal samples and inoculum, with 190 genes whose transcription levels were significantly affected in the adult digestive condition and up to 208 genes in the child.

Most of the differentially expressed genes (DEGs) detected in samples collected from the stomach between 0 and 20 min and compared to the inoculum were found upregulated: 18/22 or 20/22 for child or adult, respectively, with 14 genes shared by both age conditions (Fig. 4.C, Additional files 4 and 5). An analysis of enriched gene ontology (GO) performed on these over-expressed genes in the stomach of the child condition found two significantly enriched GO terms related to cellular components (Additional files 4 and 6.A): ribonucleoprotein complex (FDR=0.026) and ribosome

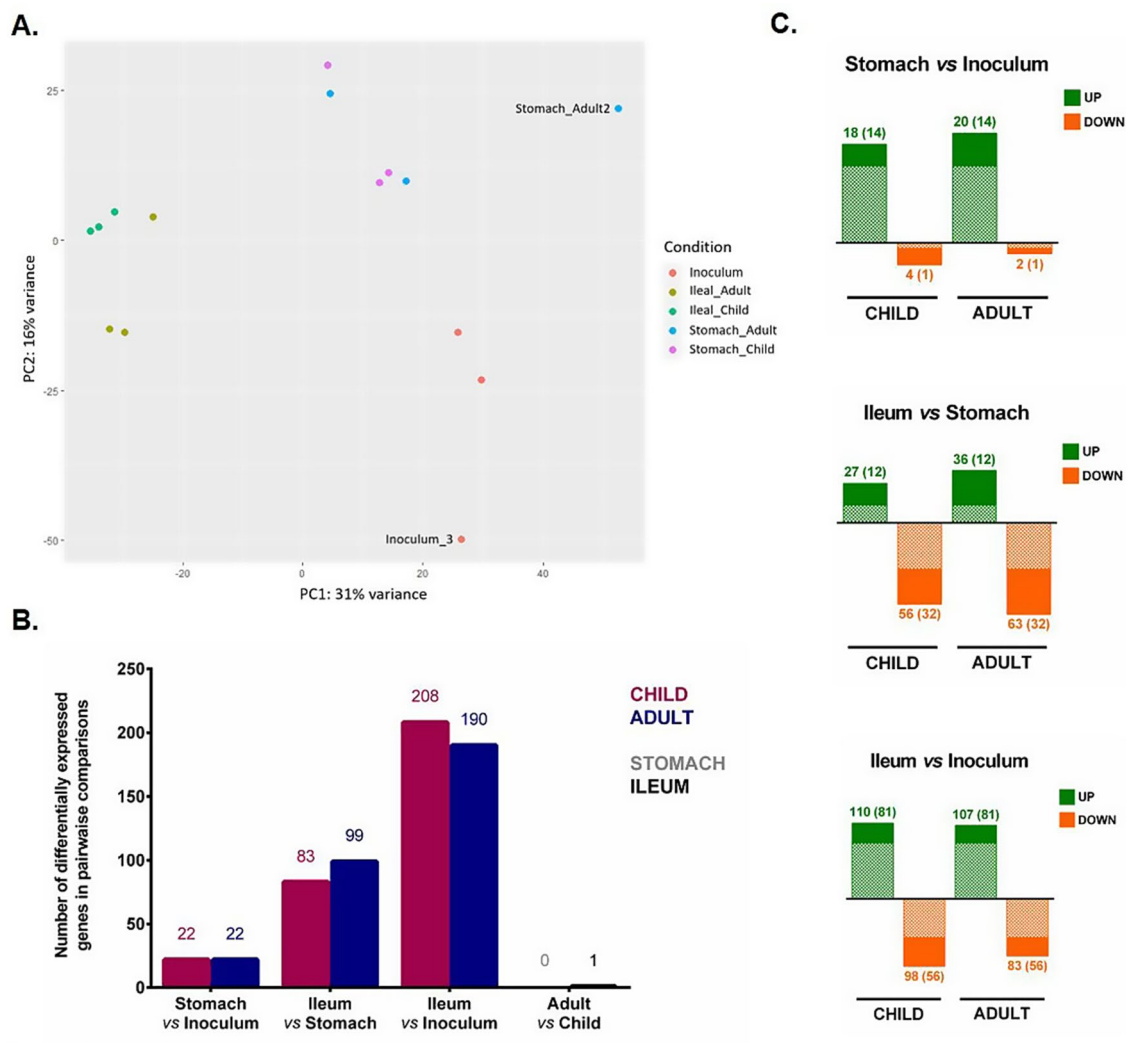


Fig. 4 RNA-Seq analysis of *C. parvum* genes in TIM-1 samples. **(A)** Principal component analysis of RNA-Seq samples investigating gene expression changes in *C. parvum* parasites collected in the inoculum ($t=0$ min), or in gastric (0–20 min) or ileal effluents (120–180 min) during the simulated child or adult digestions in the TIM-1. PCA was performed using normalised RNA-Seq data of a set of 2430 filtered genes. **(B)** Number of differentially expressed genes (DEGs) between pairwise comparisons. All DEGs show an adjusted P -value < 0.05 and a minimal regulation of 2-fold ($\log_2FC > 1$). **(C)** Number of upregulated (green) or downregulated (orange) genes between samples collected from different TIM-1 compartments in both child and adult conditions. The number of DEGs shared by age conditions is shown in brackets and with the dotted filling pattern

(FDR=0.026), both associated with the translation process. Approximately two thirds (i.e., 67.4% or 63.6% for child and adult conditions, respectively) of the DEGs identified in ileal samples compared to gastric samples were found downregulated (Fig. 4.C, Additional files 7 and 8). Thirty-two significantly downregulated genes are shared by child and adult conditions, among which a gene encoding a myosin motor domain containing protein (Gene ID CPATCC_0009620) showed a 6-fold decrease. One gene encoding an actin protein (Gene ID CPATCC_0025920) showed a 3.8-fold decrease, but only in the child condition. Among downregulated genes, GO enrichment analysis revealed a single significantly enriched GO term related to a molecular function in the adult condition: protein tyrosine/serine/threonine

phosphatase activity (FDR=0.024). Six genes that were found significantly upregulated in the child ileum compared to the child stomach encode putative secreted proteins, of which two are part of the SKSR family (Gene IDs CPATCC_0030860 and CPATCC_0035410) and one is an alpha/beta hydrolase (Gene ID CPATCC_0025460), the latter being also significantly upregulated in the adult condition. The GO enrichment analysis found six significantly enriched GO terms in the child (FDR <0.05), all related to diverse cellular components (i.e., nuclear or organelle compartments) (Additional files 6.B and 7). The expression of a gene encoding an actin family protein showed a 40-fold significant increase in the adult condition (Gene ID CPATCC_0036850).

As mentioned above, the strongest modification of the parasite transcriptome was observed for ileal samples between 120 and 180 min of digestion when compared to the initial inoculum (Fig. 4.B, Additional files 9 and 10). For instance, 98 and 83 DEGs were significantly downregulated in child and adult ileum, respectively, with 56 genes shared by both age conditions (Fig. 4.C). Among shared downregulated genes, the expression of the gene CPATCC_0009860 encoding the cryptosporidial mucin, also designated as glycoprotein-900 (GP900), was significantly decreased by a 4.8-fold. The myosin motor domain containing protein-encoding gene CPATCC_0009620 was also significantly downregulated in the ileum compared to the inoculum (9.7- or 6.8-fold decrease in the child or the adult condition, respectively). Subsequent metabolic pathway enrichment analysis interrogating the KEGG pathway database with significantly downregulated genes highlighted glycolysis/gluconeogenesis as the single significantly enriched pathway in the child ileum (FDR=0.029) (Fig. 5.A). The expression of 110 and 107 genes was significantly increased in child and adult ileum, respectively, among which the majority (i.e., 81 genes) was shared by both age conditions (Fig. 4.C). For example, four genes encoding putative secreted protein were

significantly upregulated in both child and adult ileum, when compared to the inoculum. Among those genes, one relates to the putative secreted alpha/beta hydrolase previously identified (Gene ID CPATCC_0025460) and two belong to the SKSR gene family (CPATCC_0000030 and CPATCC_0030860). GO enrichment analysis performed on significantly upregulated genes highlighted 22 significantly enriched GO terms (FDR<0.05) shared by child and adult (Fig. 5, Additional files 9 and 10). Among these, the top three shared enriched GO terms were associated with cellular components and identified as intracellular structure, intracellular organelle and organelle. Gene expression was shared by both age conditions and associated to 26 or 32 genes out of the 110 (23.6%) or 107 (29.9%) significantly upregulated genes detected in the child or the adult condition, respectively. Using the KEGG pathway database, folate biosynthesis was identified as the top one enriched pathway in child (FDR=0.0008) or adult (FDR=0.010) ileum compared to the inoculum, and was mostly associated with upregulated helicase-encoding genes. Interestingly, the expression of one gene associated to myosin complex and cytoskeletal motor activity (Gene ID CPATCC_0021030),

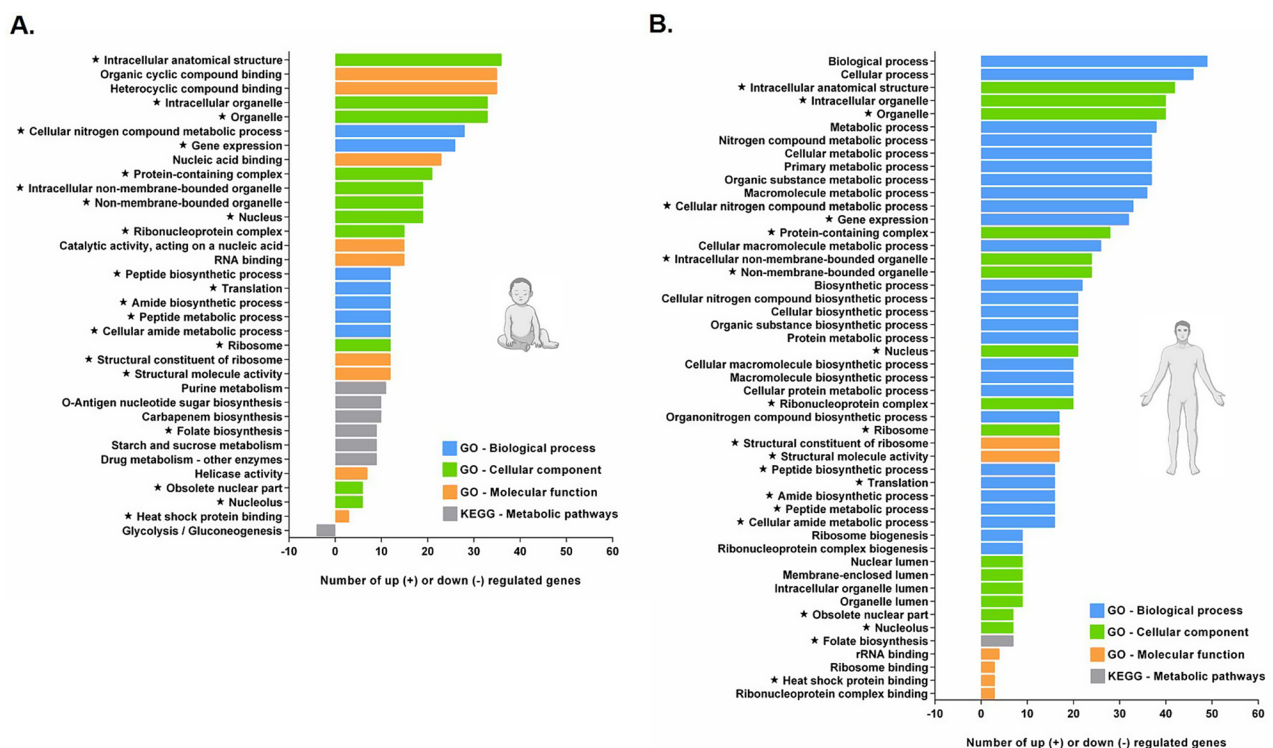


Fig. 5 Enrichment analysis on *C. parvum* genes differentially expressed in the ileal compartment. The Gene Ontology and KEGG enrichment analysis was performed on genes that were significantly up- or downregulated in the ileal effluents compared with the inoculum. The number of genes associated with each significantly enriched (i.e., showing a Benjamini-Hochberg-adjusted *P*-value or FDR < 0.05) GO term or KEGG pathway is displayed for the child (A) or the adult (B) conditions. The three GO term categories named 'Biological process', 'Cellular component' and 'Molecular function' are represented by blue, green or orange bars, respectively. The KEGG Metabolic pathways are represented by grey bars. The GO terms or KEGG pathway shared by both age conditions are indicated by a star

was highly significantly upregulated by a 1978-fold in the child ileum, compared to the inoculum sample.

Discussion

Due to the inherent limitations of in vivo experimentation within the host, the investigation of *C. parvum* excystation has only been performed to date with highly simplified in vitro approaches integrating only a few digestive parameters simultaneously (e.g., temperature, pH) [29]. Furthermore, these approaches have never been conducted under finely defined child vs. adult digestive conditions, nor combining digestive physicochemical properties with transit dynamism. Our study using the dynamic multicompartmental TIM-1 model demonstrates for the first time that most oocysts are found intact in the simulated human stomach compartment 45 min after inoculation in the TIM-1 and that the excystation step occurs rapidly and is almost completed within the following 15 min and upon passage in the duodenal compartment. These data suggest that the majority of *C. parvum* oocysts do not undergo excystation until reaching the duodenum, thereby avoiding premature release and subsequent inactivation of the more susceptible sporozoite stages in the gastric acid environment. This is in accordance with the existence of two *Cryptosporidium* lineages that show adaptation to different excystation conditions, one displaying gastric tropism including parasite species that multiply in this gastric acidic environment (e.g., *C. andersoni* and *C. muris*) and one exhibiting intestinal tropism (e.g., *C. parvum* and *C. hominis*) [30]. In order to maximise the delivery of sporozoites according to species tropism, excystation is thus activated by different host-derived triggers. In the TIM-1 system, mirroring in vivo situations, the excystation of *C. parvum* oocysts might have been triggered first by elevation of the temperature to 37 °C upon parasite inoculation into the system, followed by a drastic change in pH upon passage from the acid gastric compartment to the alkaline duodenal one. Previous in vitro studies investigating host-derived factors triggering *C. parvum* oocysts excystation have reported that temperature increase and pH change play the most important roles in the transduction of external signals across the oocyst wall to sporozoites [29, 31–33]. The digestive secretions (i.e., bile salts, trypsin and pancreatic juice) that the duodenal compartment receives in the TIM-1 system might also play a role in *C. parvum* excystation process, although our knowledge of their precise role as excystation triggers or putative synergistic effect is still limited. Interestingly, in vitro incubation of oocysts in bile, in particular in sodium taurocholate following exposure to an acid pre-treatment, has been shown to enhance parasite excystation, mimicking transition from the acidic gastric environment to the alkaline small intestine [29, 31, 34].

Our flow cytometry analysis suggests that the excystation rate was slightly more efficient along the simulated small intestine compartments upon adult digestive condition compared to the child one. This could be attributable to specific differences in the physicochemical parameters described for child versus adult physiology in a healthy state, which were subsequently implemented into the TIM-1 programs (Table 1). For instance, the discrepancy in excystation success may be explained by the slower and less pronounced gastric pH acidification in children [35, 36] and/or by the lower concentrations of various secretion components delivered in the child's duodenum, especially of bile salts [37, 38] known to enhance excystation [29, 31, 34].

The constitutively expressed luciferase marker was used as an indicator to assess sporozoite physiological state, since the intensity of its robust and sensitive signal correlates directly with the number and viability of parasites (Additional file 1). Taken together, our flow cytometry and luciferase analyses suggest that the highest amount of released sporozoites is present in the simulated ileum, and their physiological state peaks in this compartment at 180 min of digestion, regardless of age conditions. This suggests that *C. parvum* has evolved an excystation process that ensures the accumulation of the maximum number of freshly released sporozoites in the gastrointestinal segment where this species shows the highest tissue tropism in vivo. While *C. parvum* has been reported to colonise both proximal intestinal segments and the colon in different hosts [39, 40], infections associated with this species are predominantly concentrated in the distal small intestine [41, 42]. For instance, recent in vivo bioluminescent imaging of a Nluc-expressing *C. parvum* strain throughout the intestinal tract of IFN- γ -KO mice clearly showed the parasites to be mainly localised in the ileum section as well as in the caecum [43].

Our results also suggest that simulated small intestine of the child condition is associated with fewer sporozoites on the one hand, but a significantly higher sporozoite luciferase activity on the other hand compared to the adult condition. Consequently, sporozoites residing in the intestinal tract of infants could be characterised by a higher viability or be in a less damaged state. In the context of a contamination by the major food- or waterborne pathogen enterohemorrhagic *Escherichia coli* (EHEC O157:H7 serotype), Roussel et al. used a similar TIM-1 setup to demonstrate that a higher amount of viable bacterial cells may reach the distal parts of the child's small intestine, compared to those of adults [12]. These results might be attributed to less stringent conditions encountered by bacteria or *C. parvum* sporozoites in the child's intestinal tract, in regard to the two-fold lower concentration in bile salts and pancreatic secretions described for children compared to adults [37, 38, 44, 45], also

reproduced in the TIM-1 model. To our knowledge, the direct impact of various concentrations of duodenal secretions on *C. parvum* sporozoite survival has not yet been investigated. Therefore, we can not exclude that the significantly decreased physiological state observed for the sporozoites released in the adult small intestine may be the result of the detergent properties associated with higher concentrations of duodenal secretions encountered in this environment (Table 1).

We then aimed to investigate whether the higher physiological state of *C. parvum* sporozoites observed in the child intestinal tract could also correlate with an increased infectivity. To this end, the TIM-1 system was combined for the first time with a cell culture assay, wherein we tested the capacity of sporozoites collected from the digestive compartments to invade human intestinal epithelial cells. The invasion assay suggests that sporozoites collected from the ileal compartment at 180 min of digestion have a significantly higher ability to invade HCT-8 cells, compared to other time points. This finding may reflect the slightly higher amount of sporozoites present in the ileum compartment, as compared to the duodenum compartment for instance, but it may also be linked to the significantly higher sporozoites' physiological state and further emphasizes the tropism of *C. parvum* for the ileum in vivo. Interestingly, when collected from the same TIM-1 compartment, but at the end of the digestion process (300 min of digestion), sporozoites show a decreased luciferase activity and demonstrate a markedly reduced ability to invade host cells. In the literature, *C. parvum* sporozoites have been reported as somewhat fragile [46–48], surviving only for a few hours after release from the much more resilient oocyst stage. Our results are in agreement with this description and suggest that the infectivity potential of these vulnerable parasite stages may decrease drastically in the small intestine lumen if invasion of epithelial cells does not occur quickly after excystation. Our invasion assay shows that, although a lower amount of sporozoites was inoculated to host cells under the child condition (i.e., according to our flow cytometry data), these sporozoites exhibit equivalent or even significantly higher invasion ability compared to the adult condition, most likely due to their “better” physiological state. Thus, our results suggest that age-related variability in digestive physicochemical parameters may modulate different features of sporozoite physiology, and therefore participate in higher susceptibility of young children to *C. parvum* infection compared to adults.

In this study, we also aimed to characterise the modulation of the *C. parvum* gene expression in response to the various digestive physicochemical parameters encountered by the parasite in two different compartments of the child or adult gastrointestinal tract. Intriguingly, our

results revealed that the parasite transcriptome is almost exclusively affected by the time and/or compartment of digestion in the TIM-1, rather than by the simulated age (i.e., child vs. adult). This observation suggests that parasite gene expression is predominantly governed by the succession of shifts in digestive environmental conditions and the duration of digestion, rather than by more subtle physicochemical specificities associated with age condition. In contrast, previous RT-qPCR analyses performed on TIM-1 gastric and ileal effluents have shown that the expression of major EHEC O157:H7 bacterial virulence genes was significantly higher under child digestive conditions, compared to the adult ones [12]. Regarding *C. parvum*, although differences in digestive physicochemical properties between infants and adults may influence the amount, physiological state and invasiveness of sporozoites released in the small intestine, they may not be associated with significant modulation of parasite genes associated with virulence.

Transcriptomic analysis performed on TIM-1 gastric effluents collected within the initial twenty minutes of digestion detected a low number of DEGs between stomach and inoculum samples, predominantly exhibiting upregulation. In this digestive compartment, where most parasites were found as intact oocysts, enrichment of upregulated genes associated with gene expression and translation was detected. Similarly, previous transcriptomic analysis has revealed that the *C. parvum* oocyst stage is highly active in protein synthesis, as evidenced by high transcripts levels of parasite genes involved in ribosome biogenesis, transcription and translation [49].

We also analysed the *C. parvum* transcriptome collected from TIM-1 ileal effluents between 120 and 180 min of digestion, when the vast majority of parasites are found as released sporozoites compared to the stomach compartment. Our RNA-Seq analysis revealed that the sporozoite-enriched transcriptome exhibited much greater modulation in the ileum compared to the stomach, with approximately 25% of upregulated genes associated with gene expression, nucleus or intracellular structures and organelles. KEGG analysis highlighted the glycolysis/gluconeogenesis as a significantly downregulated pathway in parasites collected from ileal effluents. Although *C. parvum* may possess a remnant mitochondrion, it lacks the Krebs cycle and the cytochrome-based respiration, therefore relying mainly, if not only, on glycolysis for ATP production [50]. Glycolysis-related genes are known to be highly expressed in intracellular developmental stages [51], supporting *C. parvum* replication inside host cells. While some of their related products have also been detected in the sporozoite proteome [52], they were found under-represented in this repertoire in another proteomic study [53].

Previous transcriptomic analysis has shown that, in contrast to intracellular developmental stages, *C. parvum* extracellular stages (i.e., oocysts and sporozoites) express a wider range of genes encoding specialised functions [54], with few identified orthologs outside of related parasites. Like other apicomplexan parasites, the polarised *C. parvum* sporozoites harbour unique apical secretory organelles involved in attachment, invasion, penetration and maintenance of the parasite within the host cell, (i.e., micronemes, dense granules, small granules and a single rhoptry), as well as the canonical glideosome dependent on actin and myosin providing parasite gliding motility [55–57]. Accordingly, the expression of several parasite genes associated with the latter apicomplexan feature, particularly the myosin complex and cytoskeletal motor activity, was significantly modulated in the sporozoite-enriched fractions collected from the TIM-1 ileal effluents. While two of these genes (Gene IDs CPATCC_0009620 and CPATCC_0025920) showed a moderate downregulation in these samples, two other encoding a protein from the actin family (Gene ID CPATCC_0036850) and a myosin motor domain containing protein (Gene ID CPATCC_0021030) were characterised by a tremendous 40- or ~2000-fold upregulation, respectively. Alongside this marked regulation of genes potentially related to parasite gliding motility, the expression of genes encoding putative secreted proteins was significantly modulated in ileal effluents. For instance, the expression levels of the mucin-like glycoprotein GP900 (Gene ID CPATCC_0009860) were significantly downregulated in our ileal sporozoite-enriched samples. Stored in the sporozoite micronemes and previously hypothesised to be involved in attachment and/or invasion [58], the immunodominant protein GP900 has recently been shown to enter the secretory pathway after excystation, where its short cytoplasmic domain is cleaved before discharge of the cleaved form to the extracellular space, suggesting a lubrication role during sporozoite invasion [59]. Finally, six genes encoding putative secreted proteins were significantly upregulated in the TIM-1 ileal effluents, consistent with the past detection of several proteins associated with extracellular protein secretion in the protein repertoire of *C. parvum* sporozoites [52, 53]. Apart from a predicted hydrolase, the function of these putative secreted proteins is not yet known. Interestingly, three of these genes are predicted to encode proteins belonging to the SKSR family (Gene IDs CPATCC_0030860, CPATCC_0000030 and CPATCC_0035410). This *Cryptosporidium*-specific multigene family comprises most highly polymorphic and subtelomeric genes encoding secreted proteins harbouring a signal peptide and SK and SR repeats [60]. Although present in all major human-infecting *Cryptosporidium* species, differences in the presence or absence, as well

as in the copy numbers of this subtelomeric gene family, were recently identified between sequenced *Cryptosporidium* genomes by comparative genomic analyses, similarly to two other families encoding the MEDLE secretory proteins, named after their conserved sequence motif at the C-terminus, and insulinase-like proteases [61–66]. Recent findings identified SKSR1 as a member of the secretory proteins [67] in the newly identified small granules organelles [57]. Additionally, SKSR1 was shown to be secreted into the parasite-host interface (i.e., parasitophorous vacuole membrane and feeder organelle) and to be important for *C. parvum* pathogenicity, suggesting that it may act as a virulence factor through regulating host responses [67]. More comparative studies are needed to fully elucidate the function of all SKSR members, since gene gains and losses of this subtelomeric gene family are suggested to contribute to differences in pathogenicity and host specificity in *Cryptosporidium* populations.

Conclusions

Being one of the most common causes of infectious moderate-to-severe diarrhoea in young children, cryptosporidiosis is an important contributor to early childhood mortality in low-resource settings. Using the sophisticated TIM-1 in vitro gastrointestinal model, we showed that the digestive physicochemical parameters encountered in the child digestive tract could be associated with fewer, however potentially more active and invasive sporozoites released. Our results suggest that age-mediated variation in the human gastrointestinal physiology could partially explain why infants and toddlers are more at risk. Understanding the interactions between *C. parvum* infection and various digestive components of young individuals, including physicochemical parameters, mucus barrier, and microbiota, can provide us with a more accurate picture of children susceptibility, and possible valuable information towards new treatment strategies.

Abbreviations

| | |
|---------------------|--|
| ATP | Adenosine triphosphate |
| <i>C. andersoni</i> | <i>Cryptosporidium andersoni</i> |
| <i>C. hominis</i> | <i>Cryptosporidium hominis</i> |
| <i>C. muris</i> | <i>Cryptosporidium muris</i> |
| <i>C. parvum</i> | <i>Cryptosporidium parvum</i> |
| DEG | Differentially expressed gene |
| DNA | Deoxyribonucleic acid |
| DNase | Deoxyribonuclease |
| <i>E. coli</i> | <i>Escherichia coli</i> |
| EHEC O157:H7 | Enterohemorrhagic <i>Escherichia coli</i> serotype O157:H7 |
| FBS | Fetal bovine serum |
| FDR | False discovery rate |
| GO | Gene ontology |
| GP900 | Glycoprotein-900 |
| IFN- γ | Interferon gamma |
| KEGG | Kyoto encyclopedia of genes and genomes |
| KO | Knock-out |
| Nluc | Nanoluciferase |
| PBS | Phosphate-buffered saline |

| | |
|---------|---|
| PCA | Principal component analysis |
| RLU | Relative light unit |
| RNA | Ribonucleic acid |
| RNA-Seq | RNA sequencing |
| RPMI | Roswell Park Memorial Institute |
| SEM | Standard error of the mean |
| TIM-1 | TNO (Toegepast Natuurwetenschappelijk Onderzoek) gastrointestinal model-1 |

Supplementary Information

The online version contains supplementary material available at <https://doi.org/10.1186/s13099-024-00648-2>.

Supplementary Material 1: Title of data. Luciferase activity expressed by live or heat-killed *C. parvum* INRAE Nluc parasites. **Description of data.** Luciferase activity expressed by live or heat-killed *C. parvum* INRAE Nluc parasites. Luciferase activity was measured in live (i.e., maintained at room temperature for 30 min, blue dots) or heat-killed (i.e., maintained at 60 °C for 30 min, red dots) *C. parvum* INRAE Nluc parasites, following excystation of 1×10^7 oocysts or 1×10^6 oocysts. Individual values from five independent experiments are represented. Significant differences between groups determined by Mann-Whitney non-parametric test are indicated as follows: ** $P < 0.01$. Cp, *Cryptosporidium parvum*. RT, room temperature.

Supplementary Material 2: Title of data. RNA-Seq Stomach Adult vs. Stomach Child. **Description of data.** Differentially expressed genes determined by RNA-sequencing between samples collected in gastric effluents of adult and gastric effluents of child, and results from enrichment analyses performed on significantly upregulated or downregulated genes.

Supplementary Material 3: Title of data. RNA-Seq Ileal Adult vs. Ileal Child. **Description of data.** Differentially expressed genes determined by RNA-sequencing between samples collected in ileal effluents of adult and ileal effluents of child, and results from enrichment analyses performed on significantly upregulated or downregulated genes.

Supplementary Material 4: Title of data. RNA-Seq Stomach Child vs. Inoculum. **Description of data.** Differentially expressed genes determined by RNA-sequencing between samples collected in gastric effluents of child and inoculum, and results from enrichment analyses performed on significantly upregulated or downregulated genes.

Supplementary Material 5: Title of data. RNA-Seq Stomach Adult vs. Inoculum. **Description of data.** Differentially expressed genes determined by RNA-sequencing between samples collected in gastric effluents of adult and inoculum, and results from enrichment analyses performed on significantly upregulated or downregulated genes.

Supplementary Material 6: Title of data. Enrichment analysis on *C. parvum* genes differentially expressed in the stomach compared to the inoculum (A) or in the ileum compared to the stomach (B). **Description of data.** The Gene Ontology and KEGG enrichment analysis was performed on genes that were significantly up- or downregulated. The number of genes associated with each significantly enriched (i.e., showing a Benjamini-Hochberg-adjusted P -value or $FDR < 0.05$) GO term or KEGG pathway is displayed for both child (left) and adult (right) conditions. The three GO term categories named 'Biological process', 'Cellular component' and 'Molecular function' are represented by blue, green or orange bars, respectively. The KEGG Metabolic pathways are represented by grey bars.

Supplementary Material 7: Title of data. RNA-Seq Ileal Child vs. Stomach Child. **Description of data.** Differentially expressed genes determined by RNA-sequencing between samples collected in ileal effluents of child and gastric effluents of child, and results from enrichment analyses performed on significantly upregulated or downregulated genes.

Supplementary Material 8: Title of data. RNA-Seq Ileal Adult vs. Stomach Adult. **Description of data.** Differentially expressed genes determined by RNA-sequencing between samples collected in ileal effluents of adult and gastric effluents of adult, and results from enrichment analyses performed on significantly upregulated or downregulated genes.

Supplementary Material 9: Title of data. RNA-Seq Ileal Child vs. Inoculum. **Description of data.** Differentially expressed genes determined by

RNA-sequencing between samples collected in ileal effluents of child and inoculum, and results from enrichment analyses performed on significantly upregulated or downregulated genes.

Supplementary Material 10: Title of data. RNA-Seq Ileal Adult vs. Inoculum. **Description of data.** Differentially expressed genes determined by RNA-sequencing between samples collected in ileal effluents of adult and inoculum, and results from enrichment analyses performed on significantly upregulated or downregulated genes.

Acknowledgements

We would like to thank the Helixio company for the mRNA sequencing and bioinformatics analysis. We are also very grateful to Elise Courtot (UMR ISP, INRAE) for her help on statistical analysis.

Author contributions

JT, LE-M, SB-D and SL-L designed the project and the experiments. JT, LE-M, SC, AS, SD, CM and SL-L performed the experiments. JT and AS produced and purified the oocysts of the *C. parvum* INRAE Nluc strain. LE-M, SC, SD and CM performed the in vitro digestions. SL-L performed the flow cytometry analysis with the help of CB. JT performed the sporozoite luciferase activity and the cell culture experiments. AS performed the parasite RNA extractions. JT and GS analysed the RNA-Seq data. JT, LE-M, GS, FL, SB-D and SL-L interpreted the experimental work. JT, FL and SL-L secured funding. JT, LE-M, SB-D and SL-L wrote the paper with editorial support and comments from all other authors. All authors read and approved the final version of the manuscript.

Funding

This research was supported by the INRAE Animal Health division and by the Laboratoire d'Excellence (LabEx) ParaFrap (ANR-11-LABX-0024).

Data availability

The datasets generated and analysed during the current study are available in the GEO repository database, under accession number GSE271211 (<https://www.ncbi.nlm.nih.gov/geo/query/acc.cgi?acc=GSE271211>).

Declarations

Ethics approval and consent to participate

Not applicable.

Consent for publication

Not applicable.

Competing interests

The authors declare no competing interests.

Author details

¹UMR 1282 ISP, Infectiologie et Santé Publique, INRAE, Université de Tours, Nouzilly, France

²UMR 454 MEDIS, Microbiologie Environnement Digestif et Santé, Université Clermont Auvergne, INRAE, Clermont-Ferrand, France

³Centre Imagerie Cellulaire Santé, Université Clermont Auvergne, Clermont-Ferrand, France

Received: 18 July 2024 / Accepted: 23 September 2024

Published online: 01 October 2024

References

1. Checkley W, White AC, Jaganath D, Arrowood MJ, Chalmers RM, Chen XM, et al. A review of the global burden, novel diagnostics, therapeutics, and vaccine targets for *Cryptosporidium*. *Lancet Infect Dis*. 2015;15(1):85–94.
2. Kotloff KL, Nataro JP, Blackwelder WC, Nasrin D, Farag TH, Panchalingam S, et al. Burden and aetiology of diarrhoeal disease in infants and young children in developing countries (the Global Enteric Multicenter Study, GEMS): a prospective, case-control study. *Lancet*. 2013;382(9888):209–22.

3. Platts-Mills JA, Babji S, Bodhidatta L, Gratz J, Haque R, Havt A, et al. Pathogen-specific burdens of community diarrhoea in developing countries: a multisite birth cohort study (MAL-ED). *Lancet Glob Health*. 2015;3(9):e564–575.
4. Mølbak K, Højlyng N, Gottschau A, Sá JC, Ingholt L, da Silva AP, et al. Cryptosporidiosis in infancy and childhood mortality in Guinea Bissau, West Africa. *BMJ*. 1993;307(6901):417–20.
5. Khalil IA, Troeger C, Rao PC, Blacker BF, Brown A, Brewer TG, et al. Morbidity, mortality, and long-term consequences associated with diarrhoea from Cryptosporidium infection in children younger than 5 years: a meta-analysis study. *Lancet Glob Health*. 2018;6(7):e758–68.
6. Shirley DAT, Moonah SN, Kotloff KL. Burden of disease from cryptosporidiosis. *Curr Opin Infect Dis*. 2012;25(5):555–63.
7. English ED, Guérin A, Tandel J, Striemen B. Live imaging of the *Cryptosporidium parvum* life cycle reveals direct development of male and female gametes from type I meronts. *PLoS Biol*. 2022;20(4):e3001604.
8. Laurent F, Lacroix-Lamadé S. Innate immune responses play a key role in controlling infection of the intestinal epithelium by *Cryptosporidium*. *Int J Parasitol*. 2017;47(12):711–21.
9. Kaye JL. Review of paediatric gastrointestinal physiology data relevant to oral drug delivery. *Int J Clin Pharm*. 2011;33(1):20–4.
10. Uriot O, Chalancon S, Mazal C, Etienne-Mesmin L, Denis S, Blanquet-Diot S. Use of the dynamic TIM-1 model for an in-depth understanding of the survival and virulence gene expression of Shiga toxin-producing *Escherichia coli* in the human stomach and small intestine. *Methods Mol Biol*. 2021;2291:297–315.
11. Miszczycha SD, Thévenot J, Denis S, Callon C, Livrelli V, Alric M, et al. Survival of *Escherichia coli* O26:H11 exceeds that of *Escherichia coli* O157:H7 as assessed by simulated human digestion of contaminated raw milk cheeses. *Int J Food Microbiol*. 2014;172:40–8.
12. Roussel C, Cordonnier C, Galia W, Le Goff O, Thévenot J, Chalancon S, et al. Increased EHEC survival and virulence gene expression indicate an enhanced pathogenicity upon simulated pediatric gastrointestinal conditions. *Pediatr Res*. 2016;80(5):734–43.
13. Roussel C, De Paepe K, Galia W, De Bodt J, Chalancon S, Leriche F, et al. Spatial and temporal modulation of enterotoxigenic *E. Coli* H10407 pathogenesis and interplay with microbiota in human gut models. *BMC Biol*. 2020;18(1):141.
14. Roussel C, De Paepe K, Galia W, de Bodt J, Chalancon S, Denis S, et al. Multi-targeted properties of the probiotic *Saccharomyces cerevisiae* CNCM I-3856 against enterotoxigenic *Escherichia coli* (ETEC) H10407 pathogenesis across human gut models. *Gut Microbes*. 2021;13(1):1953246.
15. Cavestri C, Savard P, Fliss I, Emond-Rhéault JG, Hamel J, Kukavica-Ibrulj I, et al. *Salmonella enterica* subsp. *enterica* virulence potential can be linked to higher survival within a dynamic in vitro human gastrointestinal model. *Food Microbiol*. 2022;101:103877.
16. Sauvaitre T, Van Landuyt J, Durif C, Roussel C, Sivignon A, Chalancon S, et al. Role of mucus-bacteria interactions in Enterotoxigenic *Escherichia coli* (ETEC) H10407 virulence and interplay with human microbiome. *NPJ Biofilms Microbiomes*. 2022;8(1):86.
17. Swale C, Bougdour A, Gnahoui-David A, Tottey J, Georgeault S, Laurent F, et al. Metal-captured inhibition of pre-mRNA processing activity by CPSF3 controls *Cryptosporidium* infection. *Sci Transl Med*. 2019;11(517):eaax7161.
18. Dobin A, Davis CA, Schlesinger F, Drenkow J, Zaleski C, Jha S, et al. STAR: ultrafast universal RNA-seq aligner. *Bioinformatics*. 2013;29(1):15–21.
19. Love MI, Huber W, Anders S. Moderated estimation of Fold change and dispersion for RNA-seq data with DESeq2. *Genome Biol*. 2014;15(12):550.
20. Robinson MD, McCarthy DJ, Smyth GK. edgeR: a Bioconductor package for differential expression analysis of digital gene expression data. *Bioinformatics*. 2010;26(1):139–40.
21. Ashburner M, Ball CA, Blake JA, Botstein D, Butler H, Cherry JM, et al. Gene ontology: tool for the unification of biology. The Gene Ontology Consortium. *Nat Genet*. 2000;25(1):25–9.
22. Gene Ontology Consortium, Aleksander SA, Balhoff J, Carbon S, Cherry JM, Drabkin HJ, et al. The Gene Ontology knowledgebase in 2023. *Genetics*. 2023;224(1):iyad031.
23. Kanehisa M, Goto S. KEGG: kyoto encyclopedia of genes and genomes. *Nucleic Acids Res*. 2000;28(1):27–30.
24. Kanehisa M. Toward understanding the origin and evolution of cellular organisms. *Protein Sci*. 2019;28(11):1947–51.
25. Kanehisa M, Furumichi M, Sato Y, Kawashima M, Ishiguro-Watanabe M. KEGG for taxonomy-based analysis of pathways and genomes. *Nucleic Acids Res*. 2023;51(1):587–D592.
26. Heiges M, Wang H, Robinson E, Aurrecochea C, Gao X, Kaluskar N, et al. CryptoDB: a *Cryptosporidium* bioinformatics resource update. *Nucleic Acids Res*. 2006;34:419–22.
27. Noguchi K, Gel YR, Brunner E, Konietzke F. nparLD: an R Software Package for the Nonparametric Analysis of Longitudinal Data in Factorial experiments. *J Stat Softw*. 2012;50:1–23.
28. Konietzke F, Placzek M, Schaarschmidt F, Hothorn LA. Nparcomp: an R Software Package for nonparametric multiple comparisons and simultaneous confidence intervals. *J Stat Softw*. 2015;64:1–17.
29. Smith HV, Nichols RAB, Grimason AM. *Cryptosporidium* Excystation and invasion: getting to the guts of the matter. *Trends Parasitol*. 2005;21(3):133–42.
30. Widmer G, Klein P, Bonilla R. Adaptation of *Cryptosporidium* oocysts to different excystation conditions. *Parasitology*. 2007;134(11):1583–8.
31. Robertson LJ, Campbell AT, Smith HV. In vitro excystation of *Cryptosporidium parvum*. *Parasitology*. 1993;106:13–9.
32. Forney JR, Yang S, Healey MC. Protease activity associated with excystation of *Cryptosporidium parvum* oocysts. *J Parasitol*. 1996;82(6):889–92.
33. Okhuysen PC, Chappell CL, Kettner C, Sterling CR. *Cryptosporidium parvum* metalloaminopeptidase inhibitors prevent in vitro excystation. *Antimicrob Agents Chemother*. 1996;40(12):2781–4.
34. King BJ, Keegan AR, Phillips R, Fanok S, Monis PT. Dissection of the hierarchy and synergism of the bile derived signal on *Cryptosporidium parvum* excystation and infectivity. *Parasitology*. 2012;139(12):1533–46.
35. Omari TI, Davidson GP. Multipoint measurement of intragastric pH in healthy preterm infants. *Arch Dis Child Fetal Neonatal Ed*. 2003;88(6):517–20.
36. Koziolek M, Grimm M, Becker D, Iordanov V, Zou H, Shimizu J, et al. Investigation of pH and temperature profiles in the GI tract of fasted human subjects using the Intellicap(®) system. *J Pharm Sci*. 2015;104(9):2855–63.
37. Challacombe DN, Edkins S, Brown GA. Duodenal bile acids in infancy. *Arch Dis Child*. 1975;50(11):837–43.
38. Vertzoni M, Archontaki H, Reppas C. Determination of intraluminal individual bile acids by HPLC with charged aerosol detection. *J Lipid Res*. 2008;49(12):2690–5.
39. Vítovec J, Koudela B. Pathogenesis of intestinal cryptosporidiosis in conventional and gnotobiotic piglets. *Vet Parasitol*. 1992;43(1–2):25–36.
40. Kelly P, Makumbi FA, Carnaby S, Simjee AE, Farthing MJG. Variable distribution of *Cryptosporidium parvum* in the intestine of AIDS patients revealed by polymerase chain reaction. *Eur J Gastroenterol Hepatol*. 1998;10(10):855.
41. Current WL, Garcia LS. Cryptosporidiosis. *Clin Microbiol Rev*. 1991;4(3):325–58.
42. de Graaf DC, Vanopdenbosch E, Ortega-Mora LM, Abbassi H, Peeters JE. A review of the importance of cryptosporidiosis in farm animals. *Int J Parasitol*. 1999;29(8):1269–87.
43. Gallego-Lopez GM, Mendoza Cavazos C, Tibabuzo Perdomo AM, Garfoot AL, O'Connor RM, Knoll LJ. Dual transcriptomics to determine gamma interferon-independent host response to intestinal *Cryptosporidium parvum* infection. *Infect Immun*. 2022;90(2):e0063821.
44. Delachaume-Salem E, Sarles H. [Normal human pancreatic secretion in relation to age]. *Biol Gastroenterol (Paris)*. 1970;2:135–46.
45. Kalantzi L, Goumas K, Kalioras V, Abrahamsson B, Dressman JB, Reppas C. Characterization of the human upper gastrointestinal contents under conditions simulating bioavailability/bioequivalence studies. *Pharm Res*. 2006;23(1):165–76.
46. Arrowood MJ. In vitro cultivation of cryptosporidium species. *Clin Microbiol Rev*. 2002;15(3):390–400.
47. Matsubayashi M, Ando H, Kimata I, Nakagawa H, Furuya M, Tani H, et al. Morphological changes and viability of *Cryptosporidium parvum* sporozoites after excystation in cell-free culture media. *Parasitology*. 2010;137(13):1861–6.
48. Castellanos-Gonzalez A, Perry N, Nava S, White AC. Preassembled single-stranded RNA-Argonaute complexes: a novel method to silence genes in *Cryptosporidium*. *J Infect Dis*. 2016;213(8):1307–14.
49. Zhang H, Guo F, Zhou H, Zhu G. Transcriptome analysis reveals unique metabolic features in the *Cryptosporidium parvum* oocysts associated with environmental survival and stresses. *BMC Genomics*. 2012;13:647.
50. Abrahamsen MS, Templeton TJ, Enomoto S, Abrahante JE, Zhu G, Lancto CA, et al. Complete genome sequence of the apicomplexan, *Cryptosporidium parvum*. *Science*. 2004;304(5669):441–5.
51. Mauzy MJ, Enomoto S, Lancto CA, Abrahamsen MS, Rutherford MS. The *Cryptosporidium parvum* transcriptome during in vitro development. *PLoS ONE*. 2012;7(3):e31715.
52. Snelling WJ, Lin Q, Moore JE, Millar BC, Tosini F, Pozio E, et al. Proteomics analysis and protein expression during sporozoite excystation of *Cryptosporidium parvum* (Coccidia, Apicomplexa). *Mol Cell Proteom*. 2007;6(2):346–55.

53. Sanderson SJ, Xia D, Prieto H, Yates J, Heiges M, Kissinger JC, et al. Determining the protein repertoire of *Cryptosporidium parvum* sporozoites. *Proteomics*. 2008;8(7):1398–414.
54. Matos LVS, McEvoy J, Tzipori S, Bresciani KDS, Widmer G. The transcriptome of *Cryptosporidium* oocysts and intracellular stages. *Sci Rep*. 2019;9(1):7856.
55. Wetzel DM, Schmidt J, Kuhlenschmidt MS, Dubey JP, Sibley LD. Gliding motility leads to active cellular invasion by *Cryptosporidium parvum* sporozoites. *Infect Immun*. 2005;73(9):5379–87.
56. Guérin A, Striepen B. The biology of the intestinal intracellular parasite *Cryptosporidium*. *Cell Host Microbe*. 2020;28(4):509–15.
57. Guérin A, Strelau KM, Barylyuk K, Wallbank BA, Berry L, Crook OM, et al. *Cryptosporidium* uses multiple distinct secretory organelles to interact with and modify its host cell. *Cell Host Microbe*. 2023;31(4):650–e6646.
58. Barnes DA, Bonnin A, Huang JX, Gousset L, Wu J, Gut J, et al. A novel multi-domain mucin-like glycoprotein of *Cryptosporidium parvum* mediates invasion. *Mol Biochem Parasitol*. 1998;96(1):93–110.
59. Li X, Yin J, Wang D, Gao X, Zhang Y, Wu M, et al. The mucin-like, secretory type-I transmembrane glycoprotein GP900 in the apicomplexan *Cryptosporidium parvum* is cleaved in the secretory pathway and likely plays a lubrication role. *Parasit Vectors*. 2022;15(1):170.
60. Widmer G, Carmena D, Kváč M, Chalmers RM, Kissinger JC, Xiao L et al. Update on *Cryptosporidium* spp.: highlights from the Seventh International Giardia and *Cryptosporidium* Conference. *Parasite*. 2020;27:14.
61. Guo Y, Tang K, Rowe LA, Li N, Roellig DM, Knipe K, et al. Comparative genomic analysis reveals occurrence of genetic recombination in virulent *Cryptosporidium hominis* subtypes and telomeric gene duplications in *Cryptosporidium parvum*. *BMC Genomics*. 2015;16(1):320.
62. Isaza JP, Galván AL, Polanco V, Huang B, Matveyev AV, Serrano MG, et al. Revisiting the reference genomes of human pathogenic *Cryptosporidium* species: reannotation of *C. Parvum* Iowa and a new *C. Hominis* reference. *Sci Rep*. 2015;5:16324.
63. Feng Y, Li N, Roellig DM, Kelley A, Liu G, Amer S, et al. Comparative genomic analysis of the IId subtype family of *Cryptosporidium parvum*. *Int J Parasitol*. 2017;47(5):281–90.
64. Xu Z, Li N, Guo Y, Feng Y, Xiao L. Comparative genomic analysis of three intestinal species reveals reductions in secreted pathogenesis determinants in bovine-specific and non-pathogenic *Cryptosporidium* species. *Microb Genom*. 2020;6(6):e000379.
65. Wang T, Guo Y, Roellig DM, Li N, Santín M, Lombard J, et al. Sympatric recombination in zoonotic *Cryptosporidium* leads to emergence of populations with modified host preference. *Mol Biol Evol*. 2022;39(7):msac150.
66. Li J, Li N, Roellig DM, Zhao W, Guo Y, Feng Y, et al. High subtelomeric GC content in the genome of a zoonotic *Cryptosporidium* species. *Microb Genom*. 2023;9(7):mgen001052.
67. He W, Sun L, Hou T, Yang Z, Yang F, Wang T et al. SKSR1 identified as key virulence factor in *Cryptosporidium* by genetic crossing. *BioRxiv*. 2024;(577707).

Publisher's note

Springer Nature remains neutral with regard to jurisdictional claims in published maps and institutional affiliations.